INTERNATIONAL JOURNAL OF HYDROGEN ENERGY XXX (2017) 1–9

Available online at www.sciencedirect.com

ScienceDirect

journal homepage: www.elsevier.com/locate/he

Long term and performance testing of NaMg double salts for H_2/CO_2 separation

Guozhao Ji [a,b], *Julius Motuzas* [a], *Greg Birkett* [c], *Simon Smart* [a], *Kamel Hooman* [d], *João C. Diniz da Costa* [a,*]

[a] *The University of Queensland, FIM²Lab – Functional Interfacial Materials and Membranes Laboratory, School of Chemical Engineering, Brisbane, Qld, 4072, Australia*

[b] *School of Environment, Tsinghua University, Beijing, 100084, China*

[c] *The University of Queensland, School of Chemical Engineering, Brisbane, Qld, 4072, Australia*

[d] *The University of Queensland, School of Mining and Mechanical Engineering, Brisbane, Qld, 4072, Australia*

ARTICLE INFO

Article history:
Received 4 November 2016
Received in revised form
16 January 2017
Accepted 18 January 2017
Available online xxx

Keywords:
Double salts
H_2/CO_2 separation
CO_2 breakthrough
CO_2 uptake

ABSTRACT

This work investigates the synthesis and performance of double salts for H_2/CO_2 separation. A series of NaMg double salts were prepared based on $xMg(NO_3)_2$: yNa_2CO_3: zH_2O and characterised. The best sorbents reached CO_2 uptake of 17.9 wt% at 0.62 MPa and 375 °C. The NaMg double salts preferentially sorbed CO_2 as determined by breakthrough tests. The NaMg double salts were packed in a sorbent bed and tested for H_2/CO_2 separation at the back end of a water gas shift reactor. The space velocity had the largest impact on the performance of the sorbent bed, as increasing the space velocity from 2.16×10^{-3} to 9.51×10^{-3} s^{-1} sped up the breakthrough time by 84%. Increasing the feed gas pressure from 0.3 to 0.6 MPa reduced the breakthrough time by ~45%. The NaMg double salt sorbents were exposed for over 1000 h of continuous temperature including 28 cycles of sorption and desorption, and proved to be stable during changes of operating conditions such as flow rates and pressures.

Introduction

H_2 has many industrial applications ranging from hydrogenation of fuels and production of chemicals, to increasing the calorific value of gases, production of electrical energy and to power fuel cell vehicles. Therefore, there is a need for a downstream process to separate H_2 from CO_2, to meet commitments of a carbon-neutral economy by capturing CO_2 whilst using H_2 as a clean energy carrier [1]. There are several technologies that can be used for such a purpose, including membranes and solid sorbents at high temperature, or solvent absorption at low temperature. A number of membrane technologies have been reported for H_2/CO_2 separation including inorganic [2–5], metallic [6–10] and polymeric membranes [11,12]. However, there are still challenges in membrane technology for H_2/CO_2 separation, e.g., high temperature sealing and mechanical stability of the membranes. Another promising method is to lock the CO_2 in solid sorbents [13,14], thus producing high purity H_2. One example is using an alkali metal oxide based adsorbent by carbonation and decarbonation cycles such as CaO [15–18]. The reported CO_2 net uptake in CaO based sorbents varied between 19 and 36 wt % [19–21]. However, the performance of all reported CaO based absorbents deteriorates as the number of carbonation–decarbonation cycles increases and they require high temperatures (~900 °C) for calcination. As such, sintering

* *Corresponding author.*
E-mail address: j.dacosta@uq.edu.au (J.C. Diniz da Costa).

http://dx.doi.org/10.1016/j.ijhydene.2017.01.107

always occurs after the carbonation–decarbonation cycles [22,23].

There are also a number of materials for CO_2 capture in a mild to medium temperature range 250–450 °C [24]. In this case, the most interesting candidates are Mg based sorbents. One of the contenders is hydrotalcytes, also known as layered double hydroxides (LDH), which belong to a large group of anionic or basic clays [25]. Rodrigues' group [26,27] developed Mg–Al–CO_3 LDH-type sorbents reaching CO_2 uptakes of up to 2.2 wt% whilst further improvements on the synthesis of this sorbent by Reddy and co-workers [28,29] led to dry and wet CO_2 uptakes of 2.7 and 4.8 wt%, respectively. Further improvements were attained by adding CO_2 sorption promoters such as potassium, resulting in CO_2 uptakes increasing to ~6.2 wt% [30]. Although commendable, these CO_2 uptake values are still too low for industrial application. At a mild temperature range 120–150 °C [31,32], zeolites have shown good potential for processing syngas in units known as pressure swing adsorption (PSA) or vacuum swing adsorption (VSA) [33]. Webley and co-workers [31] used zeolite 13X in a pressure swing vacuum adsorption (PSVA) configuration with CO_2 sorption of ~6.9 wt% at 120 °C and desorption at 240 °C. Even at high syngas pressures of 35 bar, zeolite LiX together with activated carbon proved to be efficient for removing CO_2 for syngas streams [34]. However, activated carbon outperforms zeolites at high pressure operations [35].

Recently, Mg based double salts significantly enhanced CO_2 uptake and reaction kinetics [36,37]. Double salts of alkali metals and magnesium carbonate can be represented by the following formula $[(M_2CO_3)_m(2MHCO_3)_{(1-m)}]_n\ (MgCO_3)_p(MgO)_{(1-p)}\ xH_2O$, where M is an alkali metal such as Na, K, Li, $0 \le m \le 1$, $0.003 \le n \le 0.925$, $0 \le p \le 1$ and x represents the extent of hydration [38]. Several groups have attempted to synthesise double salt sorbents based on NaMg and KMg to achieve high CO_2 capacities. Generally, the synthesis process involved varying the concentration of the alkali metals, although results show some variation. KMg reached a good CO_2 uptake capacity of ~8.8 wt% [39]. NaMg based double salts have shown even higher CO_2 uptakes of ~15 wt% [40] and ~20.7 wt% [28], though the later reported variation in results for double salts, which is possibly linked to the reproducibility of the synthesis process.

In this work, we focus on H_2/CO_2 separation using double salts based on NaMg sorbent in view of their high reported CO_2 sorption capacity. The double salts were synthesised by a precipitation method containing NaMg and $NaNO_3$. Sorbent samples were fully characterised using materials analyses techniques based on varying the ratio of the alkali elements. Further, the performance of the best sorbent was continuously tested for 28 cycles over 1000 h (>43 days) as a sorbent bed. A number of conditions were investigated to determine the CO_2 breakthrough time based on space velocities and total pressure.

Experimental

Sorbent synthesis and characterisation

The NaMg adsorbents were prepared from a precipitation method from a stirred aqueous solution. $Mg(NO_3)_2{\cdot}6H_2O$ (Magnesium Nitrate Hexahydrate AR, Chem-Supply) was added to deionised water. After 30 min of mechanical stirring, Na_2CO_3 (Sodium Carbonate Anhydrous AR, Chem-Supply) was gradually add into the solution, which formed a slurry. Table 1 lists the reactants, mixing ratios and sample nomenclature. The stirring of the slurry continued for a further 2 h, followed by overnight settling, leading to the formation of magnesium carbonate ($MgCO_3$) and sodium nitrate ($2NaNO_3$). The slurry was then filtered by vacuum filtration and the collected white compound was dried in an oven at 60 °C for 12 h. In this method, the sodium carbonate is partially dissolved to exchange the carbonate with the nitrate in the magnesium nitrate, leading to the formation of double salts ($Na_2Mg(CO_3)_2$). The powder was crushed into fine particles and calcined in air for 4 h at 450 °C, with a ramping and cooling rate of 5 °C min^{-1}.

An in-house built volumetric adsorption rig (Fig. 1) was used to determine CO_2 adsorption up to 0.62 MPa. Degassing and/or CO_2 desorption was carried at 450 °C under vacuum by a rotary pump ($p < 10^{-3}$ Torr) for 2 h prior to each sorption. CO_2 sorption was carried out at 375 °C by measuring the pressures using a high accuracy MKS pressure transducer. The CO_2 sorbed quantity calculated from the equilibrium pressure and ideal gas law follows:

$$m_{ad}(g) = 44 \times \left(\frac{P_1V_1 + P_2V_2 - P_{eq}V_1 - P_{eq}V_2}{RT}\right) \quad (1)$$

where m_{ad} is the mass adsorbed (g), V_1 and V_2 are volumes (L) for vessels 1 and 2, P_1 is the initial pressure (Pa) in vessel 1 after dosing gas through valve 1 (with valve 2 closed), P_2 is the initial pressures (Pa) in volume 2 which is equal to the equilibrium pressure of the previous step and P_{eq} is the equilibrium pressure (Pa) after a period of equilibration with valve 2 open.

The X-ray diffraction (XRD) patterns of samples were analysed using a Rigaku Smartlab X-ray diffractometer at 45 kV, 200 mA with a step size of 0.02° and speed of 4°min^{-1} using a filtered Cu Kα radiation ($\lambda = 1.5418$ Å). Morphological features of the powder samples were examined using a Jeol JSM-7001F SEM with a hot (Schottky) electron gun at an acceleration voltage of 10 kV.

Sorbent testing

The separation of H_2/CO_2 was carried out using a system as schematically shown in Fig. 2. The WGS reactor operated continuously to provide both H_2 and CO_2. The excess unreacted water was captured by a condenser at 0 °C (using an ice slurry) between the WGS reactor and the CO_2 sorbent bed. The latter operated as batch CO_2 sorption/desorption in a Temperature Pressure Swing Adsorption (TPSA) process. A bypass was used to ensure that the WGS reactor was always

Table 1 – Double salt adsorbent mixing ratios.

$Mg(NO_3)_2{\cdot}6H_2O$ (g)	Na_2CO_3 (g)	H_2O (ml)	Sorbent name
29.04	36.15	900	$Mg29Na36H_2O900$
58.08	72.30	900	$Mg58Na72H_2O900$
116.16	144.60	900	$Mg116Na144H_2O900$
116.16	72.30	900	$Mg116Na72H_2O900$
116.16	144.60	1800	$Mg116Na144H_2O1800$

Please cite this article in press as: Ji G, et al., Long term and performance testing of NaMg double salts for H_2/CO_2 separation, International Journal of Hydrogen Energy (2017), http://dx.doi.org/10.1016/j.ijhydene.2017.01.107

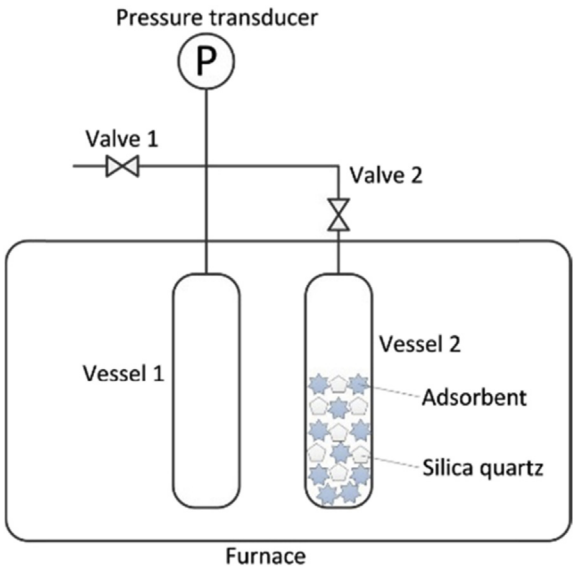

Fig. 1 – The schematic of CO_2 volumetric sorption rig.

continuously operating when it was necessary to desorb the CO_2 from the sorbent bed. The bypass stream was also used to analyse the gases generated in the WGS reactor prior to entering the CO_2 sorbent bed. Both the WGS reactor and CO_2 sorbent bed were placed in (separate) furnaces.

The WGS reactor was fed with CO and H_2O steam which reacted in the presence of WGS catalyst (Alfa Aesar™ Iron-chrome based high temperature gas shift catalyst, HiFUEL™ W210 and the reactor size is $\phi 10 \times 280$ mm) to form a syngas mixture (H_2 and CO_2). In order to increase the contact surface area, the catalyst was crushed into smaller particles with particle size $0.6 < d_p < 1$ mm. Equal weight ratio silica quartz with particle size $d_p \approx 1$ mm was mixed with the catalyst to avoid gas flow blockage. The WGS reactor contained 10 g of catalysts mixed with 10 g silica quartz, and the furnace temperature was controlled by a PID controller at desired temperatures from 460 to 580 °C. The CO feed flow ranged from 3 to 15 mL min^{-1} using flow rotameters, and water feed flow was controlled by a Bronkhorst mass flow controller at 10 g h^{-1}. The CO:H_2O molar ratio was set at 1:15 instead of 1:1 to avoid the Boudouard reaction [41–43], which leads to carbon deposition and catalyst deactivation.

The CO_2 sorbent bed contained crushed sorbents smaller than 0.1 mm and also mixed with silica quartz ($d_p \approx 1$ mm) at a ratio of 35:50 by weight, again to avoid gas flow blockage. The CO_2 sorbent bed operated at 375 °C in the sorption mode, and at 450 °C at the desorption mode. As the sorbent bed operated as a TPSA system, vacuum pressures $p < 10^{-3}$ Torr using a vacuum rotary pump was applied during the CO_2 desorption cycle. Dry gas samples were collected from the bypass and the CO_2 sorption bed outlet streams and analysed via a gas chromatography (GC) Shimadzu GC-2014. The GC was set up with a dual TCD/FID detectors and FID loop was coupled with a methanizer for CO and CO_2 detection and measurement.

Results and discussion

Sorbent characterisation

The comparison of CO_2 uptake capacity was carried out by performing two-cycles of sorption and desorption. Fig. 3 shows that the Mg58Na72H_2O900 sample reached the highest CO_2 uptake of 15 wt%. It is interesting to observe that Mg116Na144H_2O1800 has the same ratio Mg:Na:H_2O as Mg58Na72H_2O900, but has delivered a lower CO_2 uptake of 13.4 wt%. It was observed visually that the slurry of the former sample was less homogeneous than the latter sample. Doubling the amount of Mg 58 to 116 g in Mg116Na72H_2O900 almost halved the CO_2 uptake to 7.5 wt%, clearly indicating that high Mg ratio in the double salt sorbent reduced the CO_2 uptake. Doubling the water ratio also affected the reaction process, as Mg29Na36H_2O900 achieved the lowest CO_2 uptake of 4.5 wt%. These results suggest that both metal alkali ratio and the slurry formation process affect CO_2 uptake.

Fig. 4 shows the XRD patterns of samples described in Table 1, indicating the presence of Na_2CO_3 (01-077-2082), by product $NaNO_3$ (01-072-0025), the double carbonate $Na_2Mg(CO_3)_2$ (01-083-1591) and MgO (00-045-0946). The presence of Na_2CO_3 carbonates suggests that CO_2 sorption is characterised by a chemisorption at 375 °C, thus requiring a high temperature desorption cycle of ~450 °C in line with the CO_2 sorption results in Fig. 3. The presence of $NaNO_3$ in the as-prepared samples is related to the reaction of the precursors as shown in Eq. (2), which forms $NaNO_3$, whilst double salts ($Na_2Mg(CO_3)_2$) formation is represented in Eq. (3). Hence, $NaNO_3$ is a by-product and its CO_2 adsorption is negligible as reported by Lee et al. [36]. As $NaNO_3$ melting point is 308 °C, and CO_2 sorption in this work is carried out 375 °C, therefore the double salts are the compounds with significant CO_2 sorption capacity.

$$Mg(NO_3)_2 + Na_2CO_3 \rightarrow MgCO_3 + 2NaNO_3 \quad (2)$$

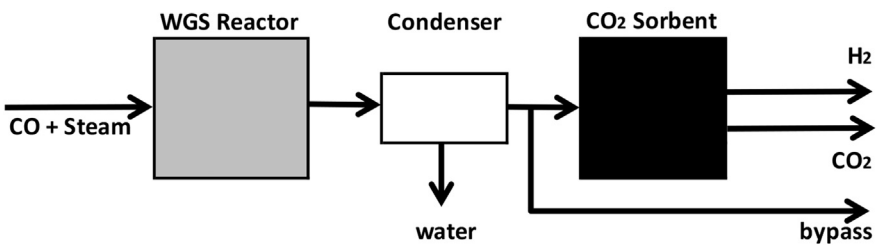

Fig. 2 – Schematic of H_2/CO_2 separation experimental rig.

Please cite this article in press as: Ji G, et al., Long term and performance testing of NaMg double salts for H_2/CO_2 separation, International Journal of Hydrogen Energy (2017), http://dx.doi.org/10.1016/j.ijhydene.2017.01.107

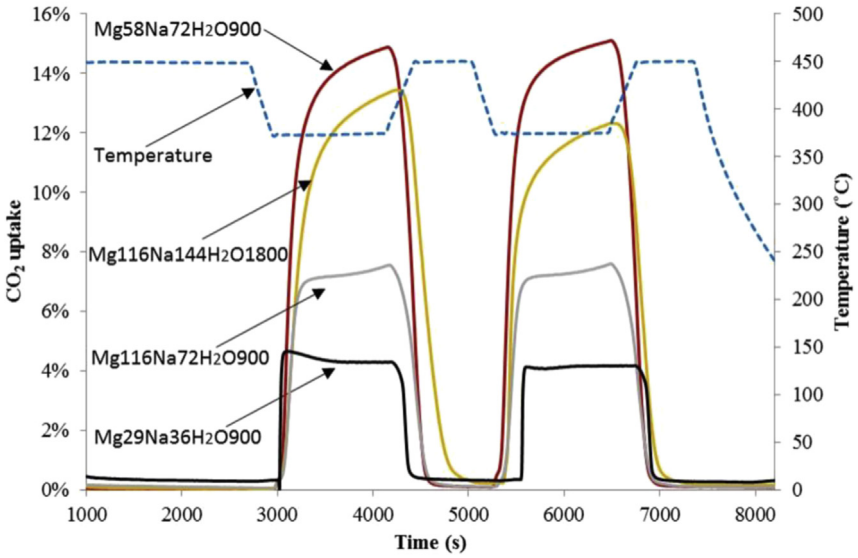

Fig. 3 – The comparison of CO_2 uptake among adsorbents from different recipes.

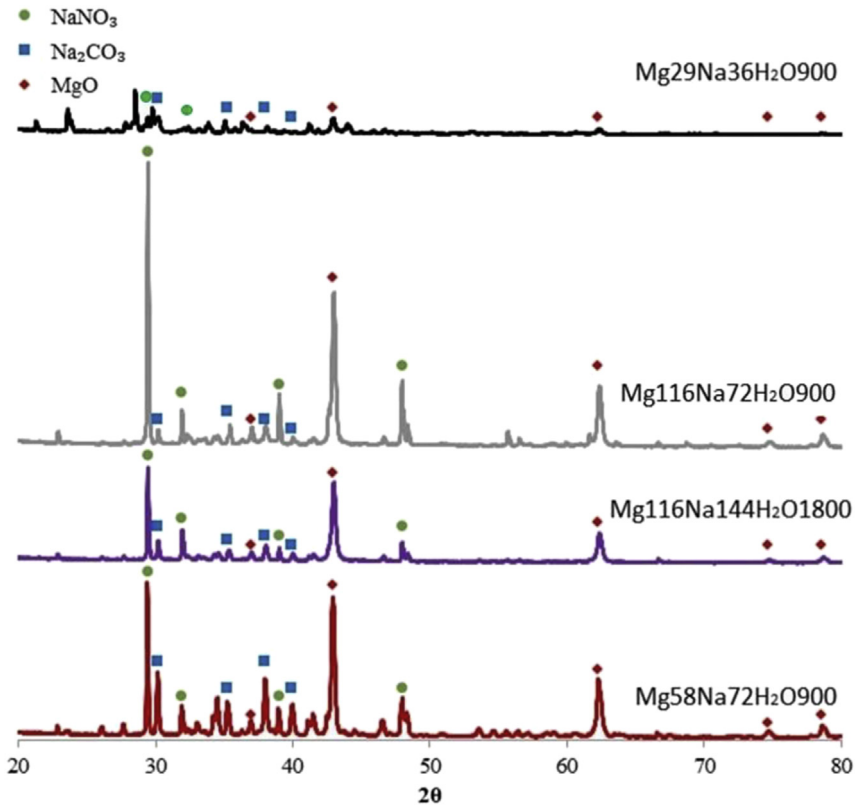

Fig. 4 – The XRD patterns of various as-prepared sorbents.

$$MgCO_3 + Na_2CO_3 \rightarrow Na_2Mg(CO_3)_2 \quad (3)$$

$$Na_2Mg(CO_3)_2 \rightarrow MgO + Na_2CO_3 + CO_2 \quad (4)$$

$$MgO + Na_2CO_3 + CO_2 \rightarrow Na_2Mg(CO_3)_2 \quad (5)$$

By applying heat, the double salt becomes a mixed material containing MgO and Na_2CO_3 whilst the chemisorbed CO_2 leaves the material structure (Eq. (4)). This is the desorption cycle, where for each mole of double salt a mole of CO_2 is desorbed. By exposing the mixed MgO and Na_2CO_3 to CO_2 at a lower temperature, CO_2 reacts forming the double salt as shown in Eq. (5). This is the chemi-sorption cycle. Essentially,

Please cite this article in press as: Ji G, et al., Long term and performance testing of NaMg double salts for H_2/CO_2 separation, International Journal of Hydrogen Energy (2017), http://dx.doi.org/10.1016/j.ijhydene.2017.01.107

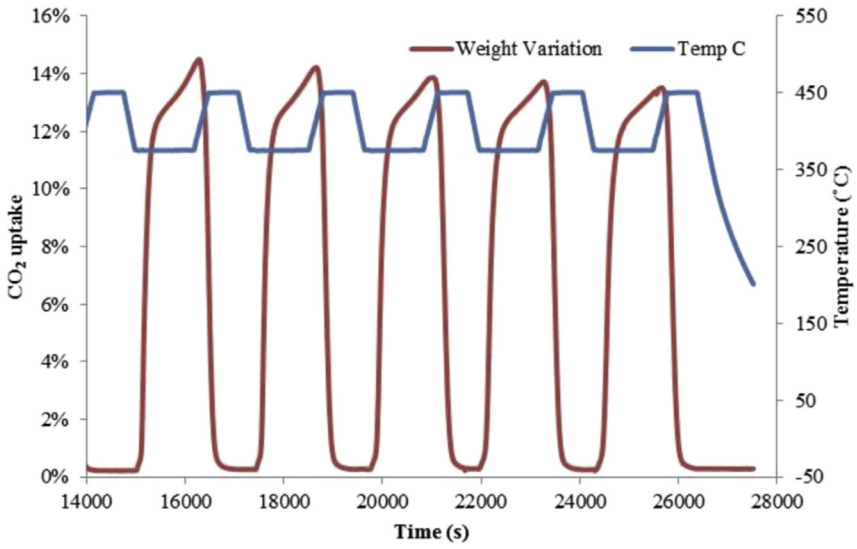

Fig. 5 – Five-Cycle test of CO_2 uptake (wt%) of $Mg58Na72H_2O900$ sorbent.

the chemi-sorption and desorption cycles are reversible, and Eqs. (4) and (5) are reverse reactions. As the double salt also contained excess $NaNO_3$, it is interesting to observe that the sample $Mg29Na36H_2O900$ with the lowest CO_2 sorption capacity in Fig. 3 has almost non-observable $NaNO_3$ peaks in the XRD patterns in Fig. 4. The other samples with superior CO_2 sorption capacity showed high intensity $NaNO_3$ peaks. As a molten salt above 308 °C, $NaNO_3$ seems to be promoting mass transfer into the double salt, in line with reports elsewhere [36].

Due to the best CO_2 uptake performance of $Mg58Na72H_2O900$, this sample was further tested for 5 thermal cycles between 370 and 450 °C for sorption and desorption, respectively. Fig. 5 shows that the initial CO_2 uptake of 15 wt% slightly decayed at every cycle, though the decay rate diminished and start stabilising by the 4th cycle, reaching 13 wt% CO_2 uptake by the 5th cycle. The retention of 87% of the CO_2 uptake capacity in the 5th cycle as compared to the initial cycle clearly indicates that CO_2 sorption is mainly reversible, a desirable property of sorbents. Initial decay is a common property of CO_2 sorbents, thus causing irreversible CO_2 sorption properties. This is generally associated with structural rearrangement during temperature cycling [43,44] attributed to sintering effect leading to loss of surface area and sorption sites [45] or reactive sites [46,47]. Further evidence on the structural re-arrangement is given in the SEM images in Fig. 6. The as-prepared sorbent (Fig. 6a) was composed of separate particles in size from 0.4 to 3 μm. After 22 cycles of CO_2 sorption and desorption, Fig. 6b shows that the particle increased in size to 1–8 μm and formed compact crystal structures.

The isothermal CO_2 uptake against pressure was also investigated for the best $Mg58Na72H_2O900$ sample. Fig. 7 shows a significant CO_2 uptake increment when the pressure was below 0.1 MPa. The CO_2 uptake increment became less noticeable for pressures >0.2 MPa. The maximum CO_2 uptake reaching 17.9 wt% obtained in this work is desirable for industrial applications. This type of isotherm has been reported by other groups [48]. This shape of isotherm is due to different CO_2 sorption sites of the double salt mixture. The CO and CO_2 partial pressures add up to 1.5 or 1.0 MPa (dry gas basis), and are common to oxygen fed [49,50] or air fed [51–53] coal gasification, respectively. Following the WGS reactor, which shifts CO to CO_2, it is expected that CO_2 uptake for these partial pressures will be in excess of 20 wt% based on the trends observed in Fig. 7.

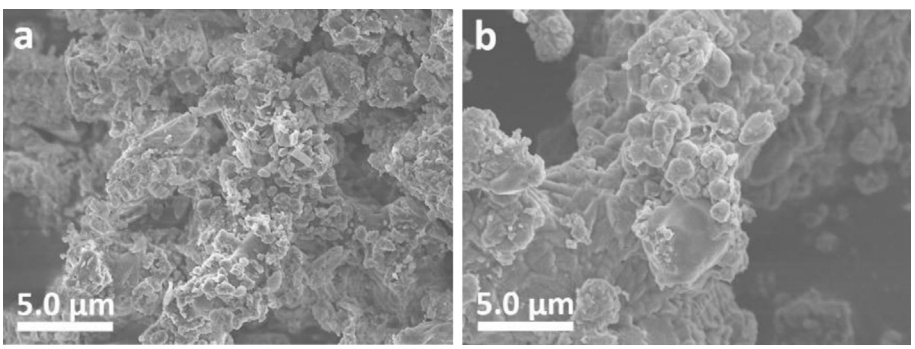

Fig. 6 – SEM micrographs of the NaMg double salt (a) as prepared and (b) after 22 CO_2 sorption/desorption cycles.

Please cite this article in press as: Ji G, et al., Long term and performance testing of NaMg double salts for H_2/CO_2 separation, International Journal of Hydrogen Energy (2017), http://dx.doi.org/10.1016/j.ijhydene.2017.01.107

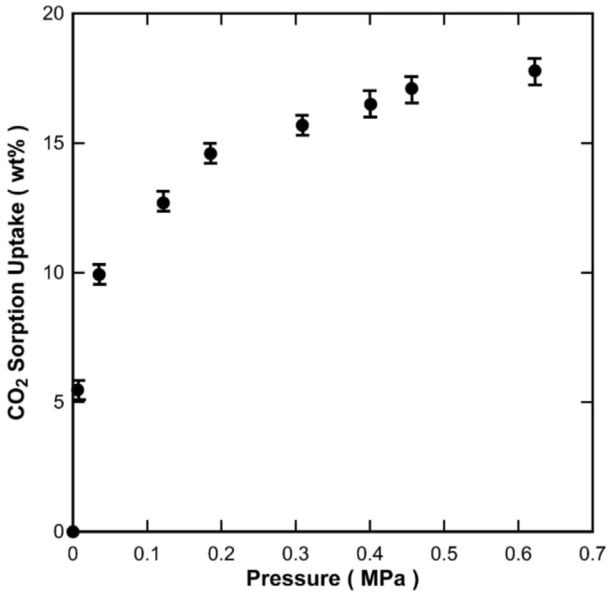

Fig. 7 – CO_2 adsorption uptake with pressure at 375 °C.

H_2/CO_2 separation

The best performing sorbent ($Mg58Na72H_2O900$) was selected for H_2/CO_2 gas separation using the TPSA experimental set up (Fig. 2). A series of experimental tests were carried out to understand the performance of the CO_2 sorbent bed by varying feed flow rates and pressures. All tests were carried out with the same sorbent for 1000 h (43 days), thus demonstrating the long term stability (28 cycles) of the best sorbent synthesised in this work. A typical representation of a CO_2 breakthrough test is shown in Fig. 8. The results show that the CO_2 concentration was <98 % up to 60 min, when it started increasing. On a similar basis the concentration of the non-adsorbing gases H_2 was just above 90% and CO ~5% (±2%) also up to the breakthrough time. The presence of CO is due to incomplete conversion of CO in the WGS reactor.

The effect of space velocity on the performance of the CO_2 sorption bed is shown in Fig. 9a. By increasing the flow rate from 3.5 to 15.4 mL min^{-1}, the CO_2 breakthrough time reduced from 190 to 30 min, a reduction of ~84%. The space velocities for these flow rates of 3.5, 6.8 and 15.4 mL min^{-1} were calculated as 2.16×10^{-3}, 4.20×10^{-3} 9.51×10^{-3} s^{-1}, respectively. The breakthrough time presents a decreasing function to space velocity or flowrate. Subsequent tests were carried out at an average syngas flow rate of ~7.0 mL min^{-1} where the pressure was varied between 0.3 and 0.6 MPa. Increasing the pressure from 0.3 to 0.6 MPa resulted in the reduction of the CO_2 breakthrough time from 90 to 50 min (Fig. 9b). This decrease is associated with equilibrium of CO_2 sorption which is non-linear, though affected by the partial pressure of CO_2 in the syngas stream.

In order to understand further the performance of the sorbent bed, the bed utilization was determined as the ratio of breakthrough time (t_{bt}) to the stoichiometry time (t_{st}):

$$Utilization = \frac{t_{bt}}{t_{st}} \tag{6}$$

$$t_{bt} = \int_0^{t_{bt}} \left(1 - \frac{F_{co_2}}{F_{co_2,\infty}}\right) dt \tag{7}$$

$$t_{st} = \int_0^{t_{\infty}} \left(1 - \frac{F_{co_2}}{F_{co_2,\infty}}\right) dt \tag{8}$$

The bed utilization results were also plotted in Fig. 9a and b as a secondary axis. The bed utilization slightly decreased from 0.68 to 0.60 as the feed flowrate significantly increased from 3.5 to 15 mL min^{-1}. The reduction in bed utilization is due to finite mass transfer and adsorption rates. With the increased flowrate, the size of the active portion of the bed increases and reduces bed utilization at breakthrough. Increasing the pressure from 0.3 to 0.4 MPa increased the bed utilization from 0.62 to 0.71. This increase derives from the higher gas concentration, which translates into increased

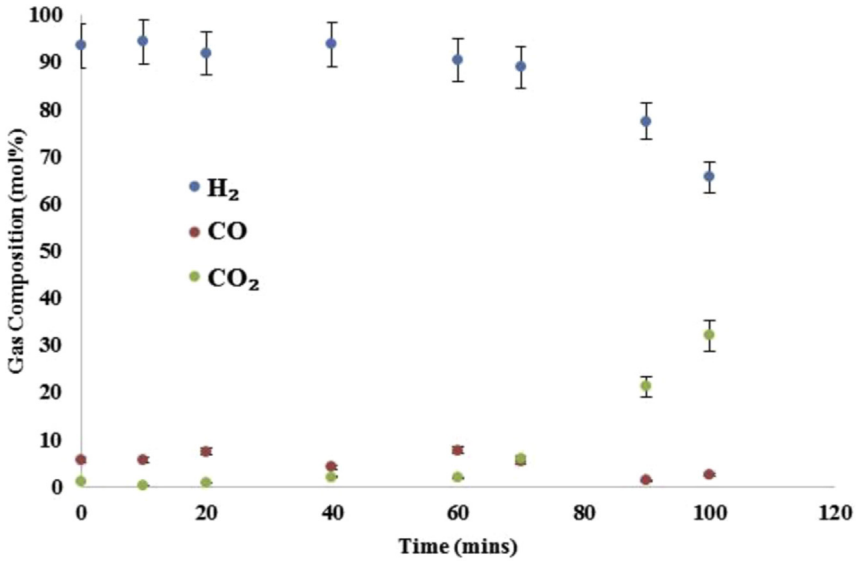

Fig. 8 – CO_2 breakthrough at: Flowrate = 7 mL min^{-1}, Pressure = 6 atm, and adsorption temperature of 375 °C.

Please cite this article in press as: Ji G, et al., Long term and performance testing of NaMg double salts for H_2/CO_2 separation, International Journal of Hydrogen Energy (2017), http://dx.doi.org/10.1016/j.ijhydene.2017.01.107

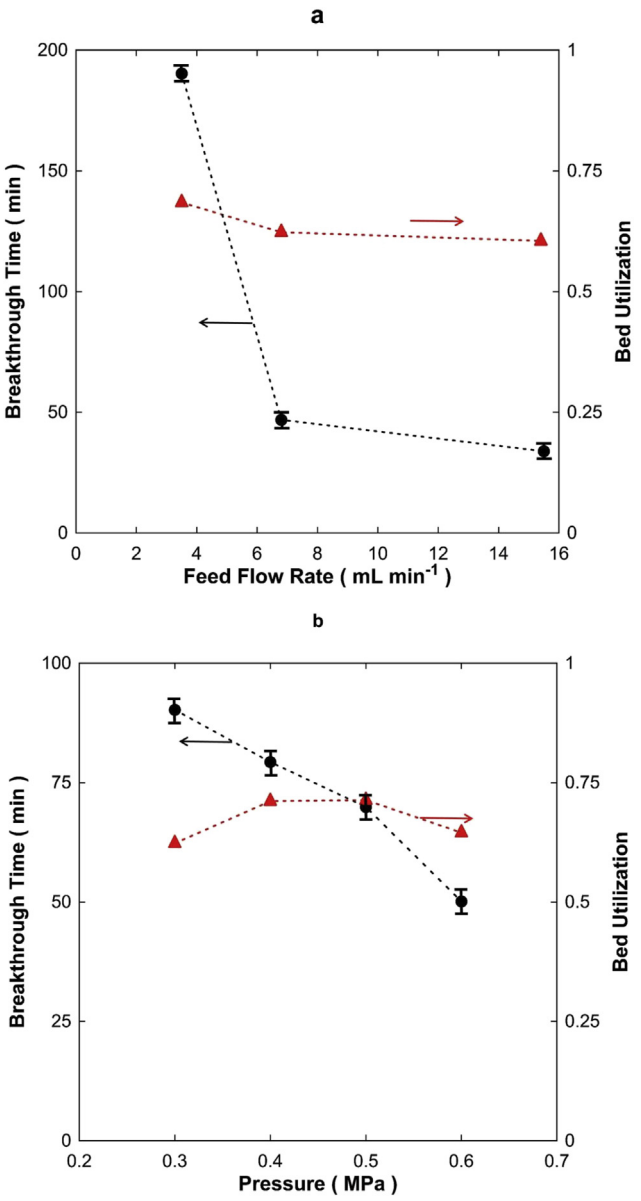

Fig. 9 – CO_2 breakthrough time and bed utilization as a function of (a) flow rates (P = 0.3 MPa) and (b) feed pressures (F = 6.8 mL min^{-1}).

mass transfer and higher CO_2 sorption. These two factors reduce the size of the active zone of the bed. This competes against the need to adsorb more CO_2 from the gas phase, which increases the size of the active zone. With pressure increased to 0.5 MPa, the bed utilization remained constant showing that the improved kinetics was balanced by the requirement for more adsorption. A further pressure increase to 0.6 MPa decreased to utilization to 0.64. These results show that the bed utilization reached a maximum point between 0.4 and 0.5 MPa due to the balance of kinetics and the amount removed from the gas phase to prevent breakthrough.

Fig. 10 shows a complete timeline of the long term performance testing in excess of over 1000 h (>43 days). The timeline had an initial region (i) where the sorbent was activated in the first day and several tests were carried out where pressure was changed from 0.1 to 0.7 MPa, and flow rates were also varied between 10 and 100 mL min^{-1}. This region also involved learning about the operating system of the experimental set up and lasted 7 days. The second region (ii) was focused on high space velocities using feed flow rates of 100 mL min^{-1} for another 7 days. It was found that the space velocities for this feed flow rate were too high for the size of the column used in this work. After region (ii) the experimental cycling work started and it was generally carried out at lower feed flow rates varying between ~5 and ~15 mL min^{-1}. Although the breakthrough varied between the highest ~193 min and the lowest ~35 min, the major limitation of this work was the GC analysis which took 30 min to analyse each point. For instance, each cycling test had up to 15 points, and

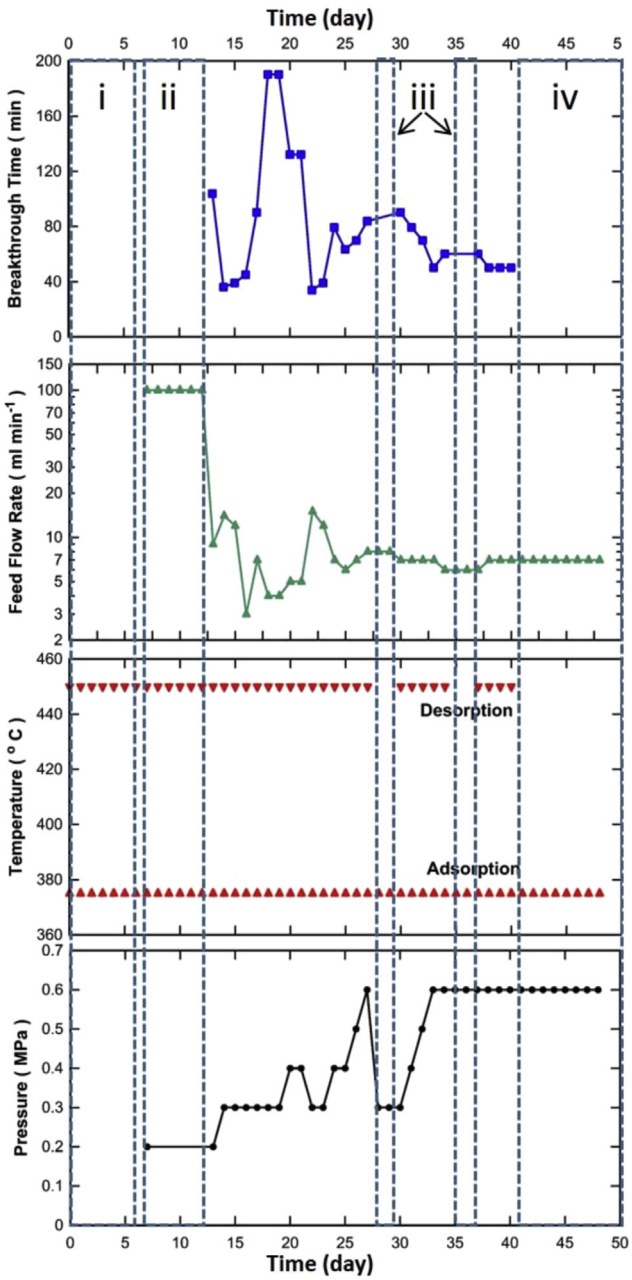

Fig. 10 – Time line of experimental work, operation conditions and breakthrough time.

Please cite this article in press as: Ji G, et al., Long term and performance testing of NaMg double salts for H_2/CO_2 separation, International Journal of Hydrogen Energy (2017), http://dx.doi.org/10.1016/j.ijhydene.2017.01.107

gas samples were collected in bags, it took up to 8 h of GC analysis to get a break through curve for a single testing condition. Region (iii) was associated with weekends where the experimental rig was left idle (no cycling work) at 375 °C and at feed flow rates of 6–7 mL min^{-1}. The last region (iv) was also left idle like region (iii). During the timeline of over 1000 h, and 28 cycling tests, the sorbents proved to be robust for H_2/CO_2 separation under the tested conditions in this work.

Conclusions

NaMg double salt sorbents proved to be suitable for separating H_2 from CO_2. In principle there is an optimised synthesis process as using too much water or Na decreases the CO_2 uptake capacity of the sorbent. The best sorbent reached a CO_2 uptake of 17.9 wt% at 0.62 MPa and 375 °C. CO_2 uptake decayed by only 2 wt% during sorption/desorption cycles and it was clear the sorbent became more stable after the 4th cycle. Further evidence of stability came from testing the sorbent over a period of 1000 h under various operating conditions to establish breakthrough times. Breakthrough curves showed that the sorbents were able to capture >98% of the CO_2 produced by the WGS reactor, thus separating H_2 from CO_2. Operating conditions were found to significantly affect the CO_2 breakthrough time, which reduced as the space velocity and CO_2 partial pressure increased. The sorbents were stable in excess of 1000 h and 28 cycles of CO_2 adsorption and desorption.

Acknowledgement

The authors wish to acknowledge financial assistance provided through Australian National Low Emissions Coal Research and Development (ANLEC R&D). ANLEC R&D is supported by Australian Coal Association Low Emissions Technology Limited and the Australian Government through the Clean Energy Initiative. The authors would also like to acknowledge the insightful comments from Mr Barry Hooper from CO2CRC and Dr Paul Feron from CSIRO. J. C. Diniz da Costa gratefully thanks the support given by the ARC Future Fellowship Program (FT130100405).

REFERENCES

[1] Muradov NZ, Veziroğlu TN. "Green" path from fossil-based to hydrogen economy: an overview of carbon-neutral technologies. Int J Hydrogen Energy 2008;33:6804–39.
[2] Criscuoli A, Basile A, Drioli E. An analysis of the performance of membrane reactors for the water-gas shift reaction using gas feed mixtures. Catal Today 2000;56:53–4.
[3] Smart S, Vente J, Diniz da Costa JC. High temperature H_2/CO_2 separation using cobalt oxide silica membranes. Int J Hydrogen Energy 2012;37:12700–7.
[4] Wang HB, Lin YS. Synthesis and modification of ZSM-5/silicalite bilayer membrane with improved hydrogen separation performance. J Membr Sci 2012;396:128–37.
[5] Battersby S, Werneck Teixeira P, Beltramini J, Duke MC, Rudolph V, Diniz da Costa JC. An analysis of the Peclet and Damkohler numbers for dehydrogenation reactions using molecular sieve silica (MSS) membrane reactors. Catal Today 2006;116:12–7.
[6] Dolan MD, Hla SS, Morpeth LD. Design and operational considerations for a catalytic membrane reactor incorporating a vanadium-based membrane. Sep Purif Technol 2015;147:398–405.
[7] Hwang K-R, Lee S-W, Ryi S-K, Kim D-K, Kim T-H, Park J-S. Water-gas shift reaction in a plate-type Pd-membrane reactor over a nickel metal catalyst. Fuel Proc Technol 2013;106:133–40.
[8] Fernandez E, Coenen K, Helmi A, Melendez J, Zuñiga J, Pacheco Tanaka DA, et al. Preparation and characterization of thin-film Pd-Ag supported membranes for high-temperature applications. Int J Hydrogen Energy 2015;40:13463–78.
[9] Koc R, Kazantzis NK, Hua Ma Y. A process dynamic modeling and control framework for performance assessment of Pd/alloy-based membrane reactors used in hydrogen production. Int J Hydrogen Energy 2011;36:4934–51.
[10] Peters TA, Stange M, Klette H, Bredesen R. High pressure performance of thin Pd-23%Ag/stainless steel composite membranes in water gas shift gas mixtures; influence of dilution, mass transfer and surface effects on the hydrogen flux. J Membr Sci 2008;316:119–27.
[11] Pesiri DR, Jorgensen B, Dye RC. Thermal optimization of polybenzimidazole meniscus membranes for the separation of hydrogen, methane, and carbon dioxide. J Membr Sci 2003;218:11–8.
[12] Scholes CA, Smith KH, Kentish SE, Stevens GW. CO_2 capture from pre-combustion processes—strategies for membrane gas separation. Int J Greenh Gas Control 2010;4:739–55.
[13] Pennline HW, Luebke DR, Jones KL, Myers CR, Morsi BI, Heintz YJ, et al. Progress in carbon dioxide capture and separation research for gasification-based power generation point. Fuel Proc Technol 2008;89:897–907.
[14] Halabi MH, de Croon MHJM, van der Schaaf J, Cobden PD, Schouten JC. High capacity potassium-promoted hydrotalcite for CO_2 capture in H_2 production. Int J Hydrogen Energy 2012;37:4516–25.
[15] Liu W, Low NW, Feng B, Diniz da Costa JC, Wang GX. Calcium precursors for the production of CaO sorbents for multicycle CO_2 Capture. Env Sci Technol 2010;44:841–7.
[16] Yan F, Jiang J, Zhao M, Tian S, Li K, Li T. A green and scalable synthesis of highly stable Ca-based sorbents for CO_2 capture. J Mater Chem A 2015;3:7966–73.
[17] An H, Song T, Shen L, Qin C, Yin J, Feng B. Coal gasification with in situ CO_2 capture by the synthetic CaO sorbent in a 1kWth dual fluidised-bed reactor. Int J Hydrogen Energy 2012;37:14195–204.
[18] Coppola A, Salatino P, Montagnaro F, Scala F. Hydration-induced reactivation of spent sorbents for fluidized bed calcium looping (double looping). Fuel Proc Technol 2014;120:71–8.
[19] Broda M, Müller CR. Synthesis of highly efficient, Ca-based, Al_2O_3-stabilized, carbon gel-templated CO_2 sorbents. Adv Mater 2012;24:3059–64.
[20] Koirala R, Gunugunuri KR, Pratsinis SE, Smirniotis PG. Effect of zirconia doping on the structure and stability of CaO-based sorbents for CO_2 capture during extended operating cycles. J Phys Chem C 2011;115:24804–12.
[21] Lu H, Khan A, Pratsinis SE, Smirniotis PG. Flame-made durable doped-CaO nanosorbents for CO_2 capture. Energy Fuels 2008;23:1093–100.
[22] Li L, King DL, Nie Z, Howard C. Magnesia-stabilized calcium oxide absorbents with improved durability for high temperature CO_2 capture. Ind Eng Chem Res 2009;48:10604–13.

Please cite this article in press as: Ji G, et al., Long term and performance testing of NaMg double salts for H_2/CO_2 separation, International Journal of Hydrogen Energy (2017), http://dx.doi.org/10.1016/j.ijhydene.2017.01.107

[23] Liu W, Feng B, Wu Y, Wang G, Barry J, Diniz da Costa JC. Synthesis of sintering-resistant sorbents for CO_2 capture. Env Sci Technol 2010;44:3093–7.
[24] Siriwardane RV, Robinson C, Shen M, Simonyi T. Novel regenerable sodium-based sorbents for CO_2 capture at warm gas temperatures. Energy Fuels 2007;21:2088–97.
[25] de Roy A, Forano C, Malki KE, Besse JP. Anionic clays: trends in pillaring chemistry. In: Expanded clays and other microporous solids. New York: van Nodrand Relohold; 2002.
[26] Yong Z, Rodrigues AE. Hydrotalcite-like compounds as adsorbents for carbon dioxide. Energy Conv Manag 2002;43:1865–76.
[27] Yong Z, Mata V, Rodrigues AE. Adsorption of carbon dioxide onto hydrotalcite-like compounds (HTLCs) at high temperatures. Ind Eng Chem Res 2001;40:204–9.
[28] Singh R, Ram Reddy MK, Wilson S, Joshi K, Diniz da Costa JC, Webley P. High temperature materials for CO_2 capture. Energy Procedia 2009;1:623–30.
[29] Ram Reddy MK, Xu ZP, Lu GQ, Diniz da Costa JC. Influence of water on high temperature CO_2 capture using layered double hydroxide derivatives. Ind Eng Chem Res 2008;47:2630–5.
[30] van Selow ER, Cobden PD, van den Brink RW, Hufton JR, Wright A. Performance of sorption-enhanced water-gas shift as a pre-combustion CO_2 capture technology. Energy Procedia 2009;1:689–96.
[31] Lee A, Xiao G, Xiao P, Joshi K, Singh R, Webley PA. High temperature adsorption materials and their performance for pre-combustion capture of carbon dioxide. Energy Procedia 2011;4:1199–206.
[32] Fisher JC, Siriwardane RV, Stevens RW. Zeolite-based process for CO_2 capture from high-pressure, moderate-temperature gas streams. Ind Eng Chem Res 2011;50:13962–8.
[33] Voldsund M, Jordal K, Anantharaman R. Hydrogen production with CO_2 capture. Int J Hydrogen Energy 2016;41:4969–92.
[34] Moon D-K, Lee D-G, Lee C-H. H_2 pressure swing adsorption for high pressure syngas from an integrated gasification combined cycle with a carbon capture process. Appl Energy 2016;183:760–74.
[35] Riboldi L, Bolland O. Comprehensive analysis on the performance of an IGCC plant with a PSA process integrated for CO_2 capture. Int J Greenh Gas Control 2015;43:57–69.
[36] Lee CH, Mun S, Lee KB. Characteristics of Na–Mg double salt for high-temperature CO_2 sorption. Chem Eng J 2014;258:367–73.
[37] Yang X, Zhao L, Xiao Y. Affecting mechanism of activation conditions on the performance of $NaNO_3$-modified dolomite for CO_2 capture. Asia Pacific J Chem Eng 2015;10:754–63.
[38] Mayorga SG, Weigel SJ, Gaffney TR, Brzozowski JR. Carbon dioxide adsorbents containing magnesium oxide suitable for use at high temperatures. USA Patent Office, Number: 6,280,503, 2001.
[39] Xiao G, Singh R, Chaffee A, Webley P. Advanced adsorbents based on MgO and K_2CO_3 for capture of CO_2 at elevated temperatures. Int J Greenh Gas Control 2011;5:634–9.
[40] Zhang K, Li XS, Duan Y, King DL, Singh P, Li L. Roles of double salt formation and $NaNO_3$ in Na_2CO_3-promoted MgO absorbent for intermediate temperature CO_2 removal. Int J Greenh Gas Control 2013;12:351–8.
[41] Geurts FWAH, Sacco Jr A. The relative rates of the Boudouard reaction and hydrogenation of CO over Fe and Co foils. Carbon 1992;30:415–8.
[42] Snoeck JW, Froment GF, Fowles M. Steam/CO_2 reforming of methane. Carbon filament formation by the Boudouard reaction and gasification by CO_2, by H_2, and by Steam: kinetic Study. Ind Eng Chem Res 2002;41:4252–65.
[43] Abanades JC, Alvarez D. Conversion limits in the reaction of CO_2 with lime. Energy Fuels 2003;17:308–15.
[44] Lysikov AI, Salanov AN, Okunev AG. Change of CO_2 carrying capacity of CaO in isothermal recarbonation–decomposition cycles. Ind Eng Chem Res 2007;46:4633–8.
[45] Sun P, Grace JR, Lim CJ, Anthony EJ. The effect of CaO sintering on cyclic CO_2 capture in energy systems. AIChE J 2007;53:2432–42.
[46] Borgwardt RH. Sintering of nascent calcium oxide. Chem Eng Sci 1989;44:53–60.
[47] Wang Q, Luo J, Zhong Z, Borgna A. CO_2 capture by solid adsorbents and their applications: current status and new trends. Energy Env Sci 2011;4:42–55.
[48] Boon J, Cobden PD, van Dijk HAJ, Hoogland C, van Selow E, van Sint Annaland M. Isotherm model for high-temperature, high-pressure adsorption of and on K-promoted hydrotalcite. Chem Eng J 2014;28:406–14.
[49] Minchener AJ. Coal gasification for advanced power generation. Fuel 2005;84:2222–35.
[50] Eftekhari AA, Wolf KH, Rogut J, Bruining H. Mathematical modeling of alternating injection of oxygen and steam in underground coal gasification. Int J Coal Geol 2015;150:154–65.
[51] Cormos C-C, Starr F, Tzimas E, Peteves S. Innovative concepts for hydrogen production processes based on coal gasification with capture. Int J Hydrogen Energy 2008;33:1286–94.
[52] Bell DA, Towler BF, Fan M. Coal gasification and its applications. Elsevier Science; 2010.
[53] Kajitani S, Suzuki N, Ashizawa M, Hara S. CO_2 gasification rate analysis of coal char in entrained flow coal gasifier. Fuel 2006;85:163–9.

Please cite this article in press as: Ji G, et al., Long term and performance testing of NaMg double salts for H_2/CO_2 separation, International Journal of Hydrogen Energy (2017), http://dx.doi.org/10.1016/j.ijhydene.2017.01.107